Ceramic industry at Morbi as a large source of SO_2 emissions in India

S. K. Kharol[1, 2]*, V. Fioletov[1], C. A. McLinden[1], M. W. Shephard[1], C. E. Sioris[1], C. Li[3, 4], and N. A. Krotkov[3]

[1] Air Quality Research Division, Environment and Climate Change Canada, Toronto, Ontario, Canada

[2] Dalla Lana School of Public Health, University of Toronto, Toronto, Ontario, Canada

[3] Atmospheric Chemistry and Dynamics Laboratory, NASA Goddard Space Flight Center, Greenbelt, Maryland, USA

[4] University of Maryland, College Park, MD, USA

Corresponding author: Shailesh Kumar Kharol (shailesh.kharol@canada.ca; shaileshan2000@gmail.com)

Key Points:

- First satellite estimates of SO_2 emissions from India's Morbi ceramic industry.
- SO_2 ceramic emissions are similar to those from large refineries and power plants.
- Morbi ceramic SO_2 emissions are ~5 times higher in 2017 compared to 2005.

Abstract

Observations from the Ozone Monitoring Instrument (OMI), onboard the NASA's Earth Observing System (EOS) Aura satellite, reveal a large SO_2 "hotspot" over Morbi, Gujarat, India, while the available emissions inventories do not report any major sources in this region. There are no industries that are typically associated with the elevated SO_2 such as large power plants, smelters, or oil refineries in the Morbi region. Our analysis shows that the elevated SO_2 source is attributed to the ceramic industries in an area of ~7 x 7 km^2 near the city. OMI-estimated SO_2 emissions from the Morbi ceramic industries have been near or above 100 kt y^{-1} since 2009, which are similar to emission levels from larger Indian oil refineries (such as Essar and Jamnagar) and power stations (such as Mundra Thermal Power Station and Ultra Mega Power Plant) located in Gujarat, India. According to OMI measurements, the SO_2 emissions from the Morbi ceramic industries are presently five times higher than they were in 2005. This study demonstrates that in the absence of any other information about SO_2 emissions from the ceramic industry, these satellite-based estimates can fill the gap in emission inventories in a timely fashion.

Keywords: sulfur dioxide, emissions, OMI, ceramic

1. Introduction

Sulfur dioxide (SO_2) is a short-lived atmospheric air pollutant emitted or formed in the atmosphere through natural and anthropogenic processes, and plays an important role in the atmospheric environment and global sulfur cycle. Once emitted SO_2 can deposit on the surface or be transformed chemically into particulate matter (i.e., sulfate aerosol). SO_2 and its oxidation products are considered as designated criteria air pollutants in many countries worldwide due to their various environmental and health consequences (Kharol et al., 2017). To supplement surface monitoring, a handful of satellite sensors have provided information on the global distribution of SO_2 since the 1990s (Krotkov et al., 2008; Li et al., 2013; Theys et al., 2015). In particular, these satellite observations are used extensively to detect anthropogenic SO_2 signals from large individual point sources such as copper and nickel smelters, power plants, oil and gas refineries, and other sources (Bauduin et al., 2016, 2014, Carn et al., 2007, 2004; de Foy et al., 2009; Fioletov et al., 2013; Lee et al., 2009; McLinden et al., 2014, 2012; Nowlan et al., 2011; Thomas et al., 2005). They can also provide information on SO_2 emissions from volcanic sources whereas other information is often not available (Carn et al., 2017). Satellite data are also used to study the evolution of SO_2 amounts over large regions such as eastern U.S. (Fioletov et al., 2015, 2011; Kharol et al., 2017), Europe (Krotkov et al., 2016), China (Jiang et al., 2012; Koukouli et al., 2016; Li et al., 2010; Witte et al., 2009), and India (Lu et al., 2013). Recently, Li et al. (2017) noticed that, with its 50% increase in SO_2 emissions since 2007, India is surpassing China and becoming world's largest emitter of anthropogenic SO_2.

As SO_2 emissions are important for air quality, emission inventories often provide estimates for them (Klimont et al., 2013), and satellite data-based emission estimates are proven to be a valuable addition to the conventional bottom-up emission inventories (Liu et al., 2018). Emissions from power plants, oil refining processes, metal ore smelting factories as well as from natural sources such as volcanoes are estimated from satellite measurements (Carn et al., 2017; Fioletov et al., 2016). Despite what is becoming an increasingly important complete global picture of SO_2 emissions, we found that a large emission source from the Indian ceramic industry near Morbi is currently missing from leading emission inventories such as Hemispheric Transport of Air Pollutants (Janssens-Maenhout et al., 2015), and can also be monitored by satellites. Ceramic products are manufactured from clays and other non-metallic inorganic materials. The clay minerals that are used as raw materials in ceramic industries often contain

high levels of sulfur. In addition, coal used in firing the ceramic products may contain sulfur that is oxidized to SO_2 in the process.

Due to high prices of natural gas, most of the ceramic industry in Morbi uses low quality coal (BEE, 2010), which is one of the major sources of SO_2 emissions. The supply of relatively inexpensive coal for ceramic industries is fulfilled by coal producing states of India (e.g., West Bengal, Jharkhand and Chhattisgarh). The increased SO_2 emissions from ceramic industries not only affect the health of ceramic workers, but also degrade the air quality in the neighboring populated areas causing deleterious health effects (Seabrook, et al., 2019) regionally and is responsible for vegetation damage (Wen, et al., 2006).

The main objective of the study is to quantify regional SO_2 emissions, with a focus on those from the ceramic industries near Morbi, India using Ozone Monitoring Instrument (OMI) satellite data. This is the first study of its kind to identify and estimate SO_2 emissions from ceramic industries. The methodology is described in section 2. Section 3 demonstrates the results of the study.

2. Data sets & Methodology

2.1. OMI Satellite observations

The Ozone Monitoring Instrument (OMI) is particularly useful for SO_2 monitoring from space. OMI is a Dutch-Finnish UV-Visible wide field-of-view nadir-viewing spectrometer flying on NASA's EOS Aura spacecraft (Schoeberl et al., 2006), providing daily global coverage at high spatial resolution (Levelt et al., 2006). The overview of OMI operation, products, science and applications has been published recently (Levelt et al., 2018). Operational OMI Planetary Boundary Layer (PBL) total column SO_2 data produced with the Principal Component Analysis (PCA) algorithm (Li et al., 2013) for the period 2005-2017 were used in this study. SO_2 vertical column densities (VCDs) (which represent the total number of molecules or total mass per unit area) are retrieved assuming PBL SO_2 profile shape and given in Dobson units (DU, 1 DU = $2.69 \cdot 10^{26}$ molec•km^{-2}). A climatological SO_2 profile over the summertime eastern U.S. was used in the retrievals (Li et al., 2013). Only clear-sky data, defined as having a cloud radiance fraction (across each pixel) less than 20%, and only measurements taken at solar zenith angles

less than 70° were used. OMI SO_2 data are retrieved for 60 cross-track positions (or rows), and the pixel ground size varies depending on the track position from 13 × 24 km² at nadir to about 28 × 150 km² at the outermost swath angle. Data from the first 10 and last 10 cross-track positions were excluded from the analysis to limit the across-track pixel width to about 40 km. Additional information on the OMI PCA SO_2 product is available from Krotkov et al. (2016).

2.2. SO_2 emission estimates

The OMI "top-down" SO_2 emission estimates used in this study are based on the multisource fitting algorithm of Fioletov et al. (2017). SO_2 values for each OMI pixel are merged with wind speed and direction from European Centre for Medium-Range Weather Forecasts (ECMWF) reanalysis data (Dee et al., 2011; http://apps.ecmwf.int/datasets/). Wind profiles are available every 6 h on a 0.75^o horizontal grid and are interpolated in space and time to the location of each OMI pixel center. The algorithm is based on fitting OMI SO_2 VCD data by a linear combination of functions of OMI pixel coordinates and wind speeds, where each function represents the plume from an individual source. It is assumed that the plume shape is the same for all sources and only the emission strength varies from source to source. The estimated total SO_2 mass (α) for each source is related to the emission strength (E). Assuming a steady state, these quantities are related through the equation $E = \alpha/\tau$, where τ is the lifetime or, more accurately, decay time. The parameter τ=6 hours was estimated from OMI data based the observed plume decay. This makes it possible to estimate emissions from these sources or groups of sources. If the location of all sources is known, it is expected that the fitting results and the actual averaged OMI data will agree within the measurement noise level (about 0.5 DU for individual pixels). It was demonstrated that the algorithm can successfully estimate emissions for the power plants in the eastern U.S., Canada and Europe (Fioletov et al., 2017). The overall uncertainty of the method is about 50%. There are several factors that contribute to the emission estimate uncertainty, however the major contributors, namely uncertainties in air mass factors (i.e., related to the optical path length through the atmosphere) and τ, appear as scaling factors. They affect emission estimates for the sources discussed in this study in the same way. In other words, even if the absolute emissions estimates may have large uncertainties, relative changes in emissions with time as well as the relative emission strength between the sources are far more accurate. The remaining factors, such as the uncertainty related to statistical errors from the regression model and errors due to incorrect wind speed and direction are about 20%.

Note that the error bars in this study represent the statistical uncertainties. Additional information about the algorithm and uncertainty analysis can be found in (Fioletov et al., 2016).

It was also demonstrated that OMI data are affected by large-scale biases that are likely related to imperfection in the removal of a very strong ozone absorption that depends on stratospheric temperature and the ozone profile. Although such large-scale biases in the OMI PCA data set are relatively small, they nonetheless can affect emission estimates. Over the Eastern U.S., a 6th order polynomial function was added to the fit to account for this large scale bias (Fioletov et al., 2017) but in this study, the analysis was performed for a much smaller area and a linear function (of latitude and longitude) was used to account for the bias that appears as a north-south gradient. The method is illustrated by Figure 1, where the 2005-2017 mean OMI SO_2 data, the fitting results, the large-scale bias, and the difference between OMI data and the fitting results (the residuals) are shown. The emission sources included in the fit are shown by the black dots. As Figure 1 shows, OMI data with the bias removed (panels a and d) agree well with the fitting results (panels b and e), giving confidence in the emission estimates.

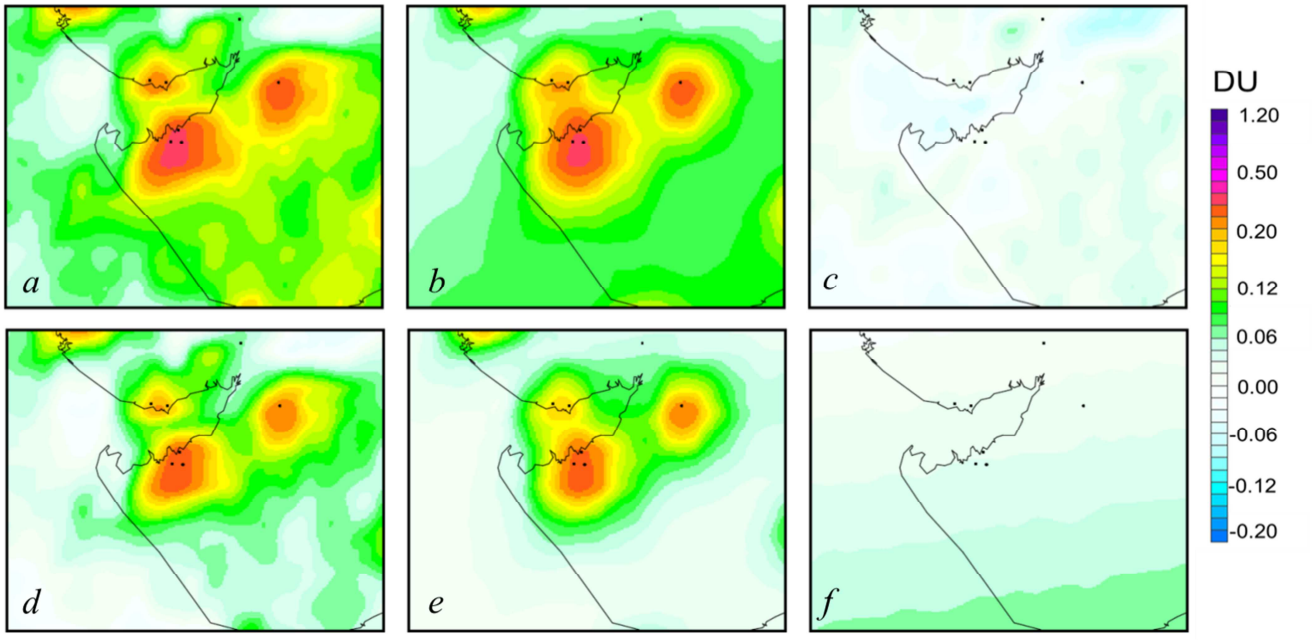

Figure 1. (a) Mean SO_2 VCDs for 2005-2017 calculated from OMI data processed with the PCA algorithm. (b) Results of the fitting of OMI data by the set of functions that represent VCDs near emission sources using estimated emissions. A linear function of latitude and longitude was added to the

fit to account for a large-scale bias. (c) The difference between OMI data and the fitting results (the residuals). (d) OMI data with the large-scale bias removed. (e) The same as (b) but without the large-scale bias. (f) The estimated large-scale bias. The maps are smoothed by the pixel averaging technique with a 30-km radius (Fioletov et al., 2011). The main industrial sources are shown by the black dots.

3. Results & Discussions

Over the past few years, ceramic tile consumption in India has increased due to the growth in average net worth of the population, a booming real estate sector along with a rapid increase in disposable income of consumers and growth in the infrastructure sector (Ernst & Young LLP, 2013). Increasing demand for ceramic products regionally and internationally resulted in an increase in ceramic production. Presently, ceramic industries in India produce ~12.9% (KICT, 2019) of global output, which places it second in the world. Morbi is the heart of India's ceramic industry, with a population of ~¼ of a million people located in the Rajkot district of Gujarat, India (Figure 2; Source 6), with over 600 ceramic manufacturing units (mostly unorganized) (Care Ratings, 2019). Approximately 80% of India's ceramic industries/factories are located in Morbi, Gujarat, India, which are mostly engaged in ceramic tiles production (e.g., wall tiles, vitrified tiles, floor tiles, roofing tiles etc.) and accounts for ~70% of India's total production of ceramic tiles (Care Ratings, 2019).

The Morbi cluster of ceramic factories expanded to ~7 x 7 km^2 in area and is clearly noticeable towards the east side of Morbi city and marked with approximate boundary in red color on the Google Earth satellite image (Figure 2, bottom panel). The proximity to key raw materials (e.g. various type of clay, red and black soil, minerals such as calcite and wollastonite) for ceramic products either locally or from a neighboring state (e.g., Rajasthan) is one of the key reasons behind Morbi being the ceramic capital of India. Apart from Morbi, there is another large Indian ceramic cluster in Thangadh, located in the Surendranagar district of Gujarat, but it is not considered here because its emissions are substantially smaller.

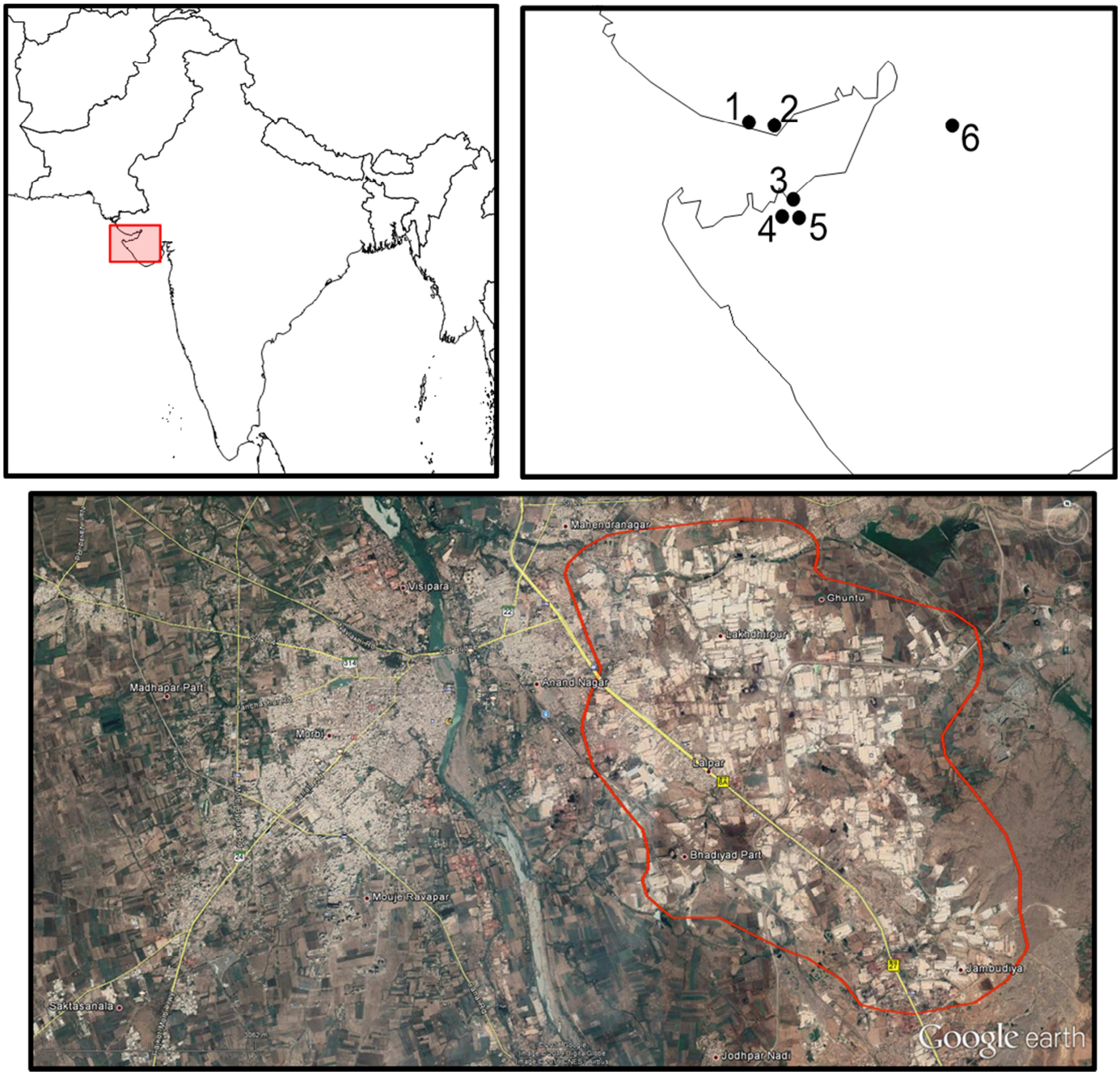

173

174 **Figure 2.** (Top left) The red square box region in Gujarat, India, analyzed in this study. (Top right) The
175 main industrial sites in the analyzed area: (1) Mundra Thermal Power Station (MTPS) and Mundra
176 Ultra-Mega Power Plant (UMPP), (2) Mundra Port, (3) Sikka Thermal Power Station, (4) Nayara
177 Energy Refinery (formally known as Essar Oil Refinery), (5) Jamnagar Oil Refinery, (6) Morbi, Gujarat,
178 India. The bottom plot is an expanded view of source (6), showing the ~7 km-wide ceramic industries
179 area within the red contour east of city of Morbi, Gujarat, India. The ceramic industries appear as white
180 rectangles on this Google Earth image.

In addition to ceramic factories at Morbi, India's second and third largest thermal power plants (namely, Mundra Thermal Power Station (MTPS) and Mundra Ultra-Mega Power Plant (UMPP)) (Power Technology, 2019), one of Gujarat's coal-fired power plant, and one of the world's largest oil refineries are located on the shores of the Gulf of Kutch (Figure 2) (World's largest refineries, 2016). Both, MTPS and UMPP are coal-fired thermal power plants and located very close to each other (~2 km apart), thus jointly considered as source 1 in Figure 1. The Mundra port (source 2, Figure 2) is the largest private port of India (Mundra Port, 2019). The Sikka Thermal Power Station (source 3, Figure 2), located near Jamnagar on the southern shore of Gulf of Kutch and operated by Gujarat State Electricity Corporation Limited (GSECL), is one of Gujarat's coal-fired power plant with two units of 250 MW (Sikka Thermal Power Station, 2019). The Nayara Energy refinery (formally known as Essar oil refinery; source 4, Figure 2) is India's second largest single site refinery located near Vadinar, Gujarat, with a capacity of 405,000 barrels per day (64,400 m^3/day) (Essar Refinery, 2019). Presently, the Jamnagar refinery (source 5, Figure 2) is the world's largest crude oil refinery owned and operated by Reliance Industries Limited, and located near Motikhavdi in Jamnagar district, Gujarat, India. It was commissioned in July 1999 with an installed capacity of 668,000 barrels per day (106,200 m^3/day) and later increased to 1,240,000 barrels per day (197,000 m^3/d) (Jamnagar Refinery, 2019).

The large changes in land use / land cover, due to the rapid industrialization in Gujarat, India, can be seen in the LANDSAT satellite True Color Composites for 1984, 2005, and 2016 (https://earthengine.google.com/timelapse/) (Figure 3). LANDSAT satellite images show large changes in the six industrial areas indicated in Figure 3. There were essentially no large industrial complexes in the six areas in 1984. By 2005 (the first year of OMI operation), Mundra port, Sikka Thermal Power station and the Jamnagar oil refinery in the Motikhavdi area were operational and some ceramic factories were seen near Morbi. The Essar oil refinery was still under construction in 2005, and completed and commissioned in 2006.

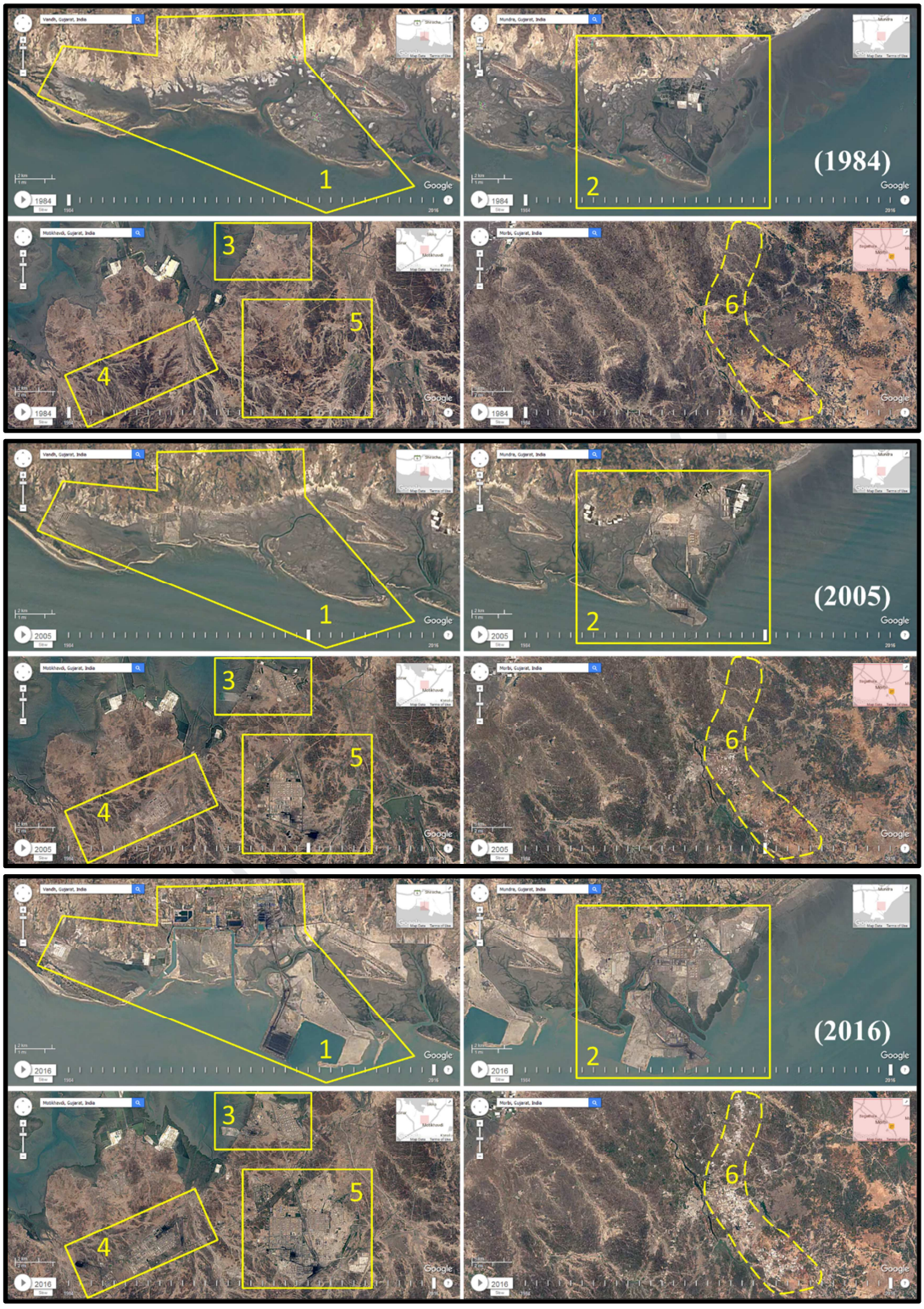

Figure 3. LANDSAT True color composites over Vandh, Mundra, Motikhavdi and Morbi, Gujarat, India for the period of 1984, 2005, and 2016. The main industrial areas, as labeled in Figure 2, are shown in each panel.

However, there was no sign of any construction activity at source 1 (i.e., MTPS and UMPP). In the bottom image for 2016, there are large industrial installations in all six areas. The construction for MTPS project began in 2008 and became fully operational in March 2012 with all nine units providing 4620 MW (4 units of 330 MW and 5 units of 660 MW) capacity (Power Technology, 2019). The first 330 MW and last 660 MW units of MTPS were commissioned in May 2009 and March 2012, respectively (Power Technology, 2019). Similarly, the construction for Mundra UMPP project began in 2007 and became fully operational in March 2013 with all five units providing 4000 MW (each of 800 MW) capacity (Power Technology, 2019). The expansion of the ceramic industrial cluster at Morbi, Gujarat is also evident in 2016.

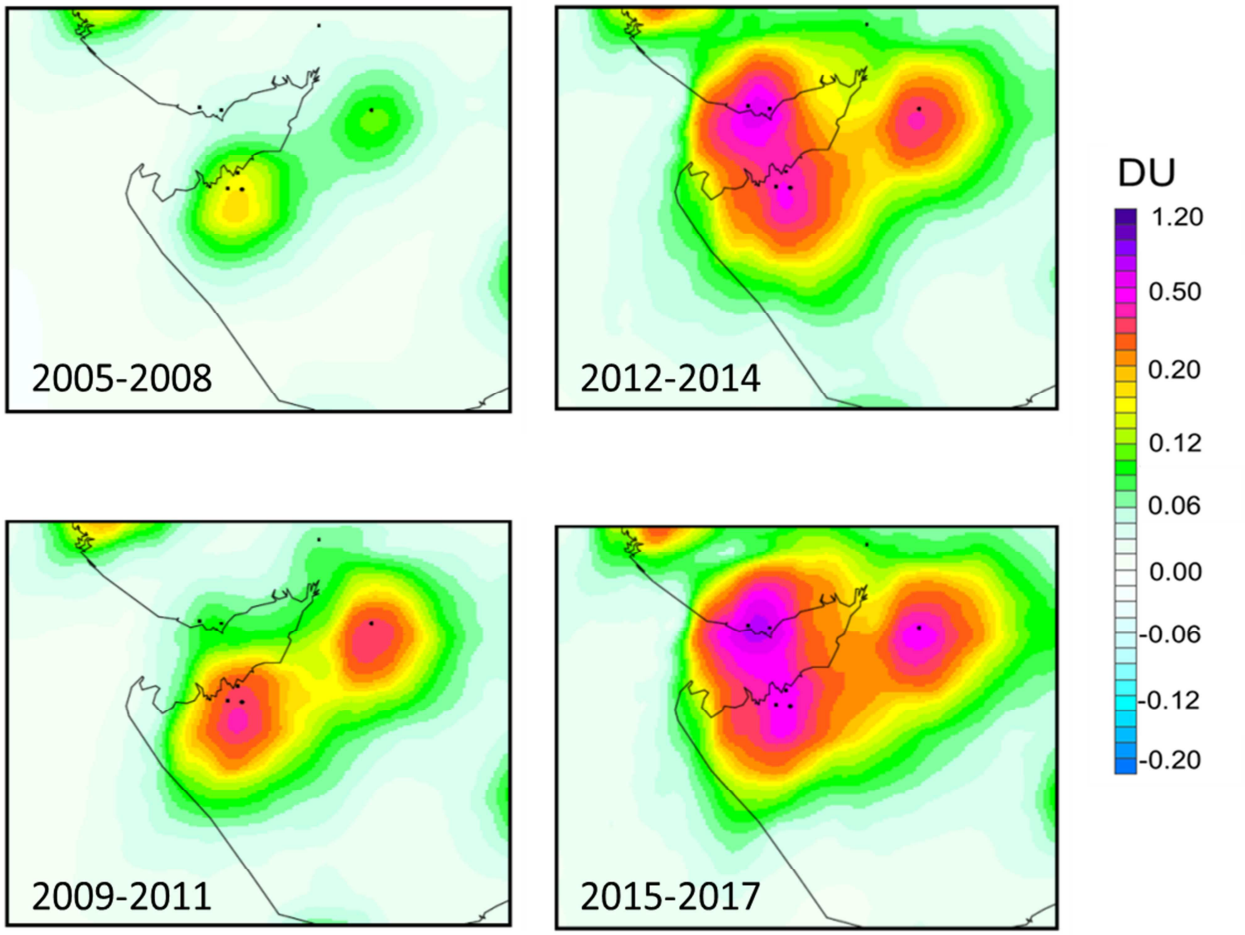

Figure 4. Mean OMI-derived SO_2 vertical column densities (VCDs) without the large-scale bias over Morbi, Gujarat, India, for the four periods as indicated on the plot. The main industrial sources are shown by the black dots.

Figure 4 shows the results of the fitting of OMI data by the set of functions that represent VCDs near emission sources using estimated emissions with the large-scale bias removed (the plot corresponds to the panel e of Figure 1). Satellite data from OMI clearly demonstrate a strong increase in SO_2 VCDs over Gujarat (Figure 4) that reflect an increase in emissions (discussed below). In 2005-2008, only some relatively weak SO_2 signals from the Jamnagar oil refinery at Motikhavdi and the Morbi ceramic cluster existed. That signal increased significantly by 2011. After 2011, elevated SO_2 VCDs were observed north of the Gulf of Kutch as the operation of the MTPS and UMPP power plants had started. The SO_2 VCDs increased over Morbi due to the expansion of ceramic cluster.

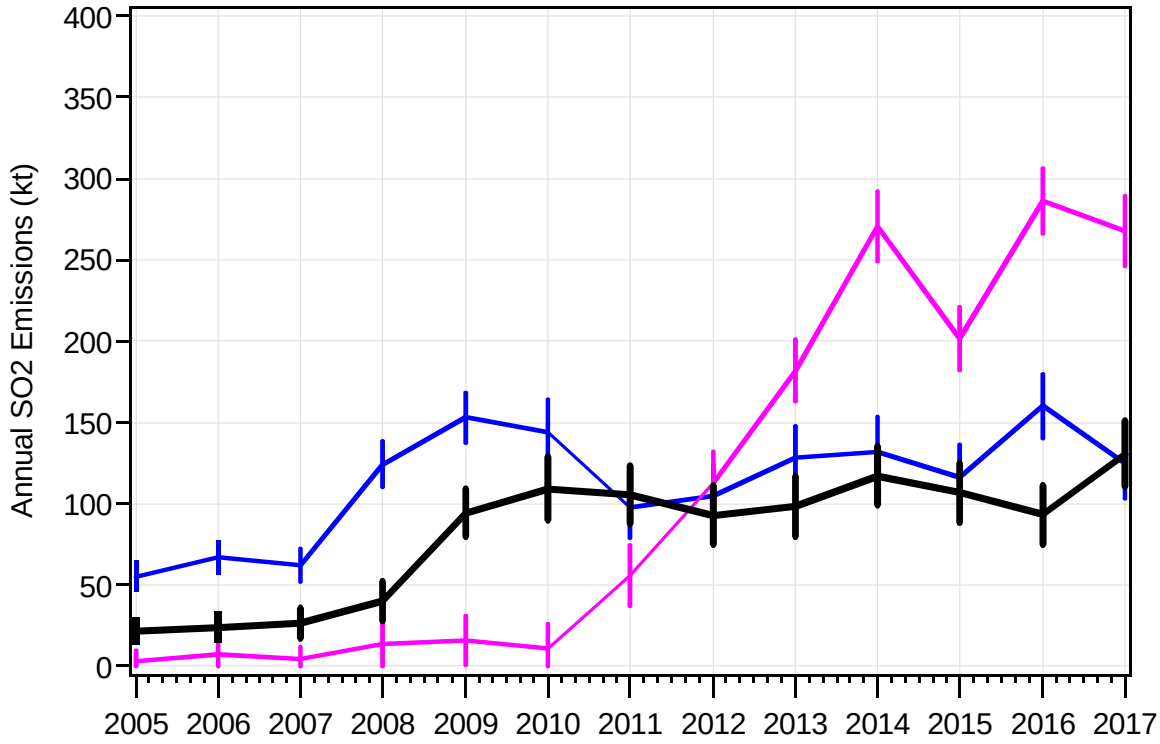

Figure 5. Annual SO_2 emissions for the three main industrial regions estimated from OMI data. The magenta line indicates emissions from the sources 1 and 2, the blue line represents the sources 3, 4, and 5, and the black line demonstrates emissions from the ceramic industry (source 6) at Morbi (see Figure 2 for source locations). The error bars represent 95% confidence intervals.

The data fitting algorithms can be used to estimate SO_2 emissions from individual factories or groups of factories located in close proximity (Fioletov et al., 2017). Figure 5 shows the estimated annual emissions from three clusters of SO_2 sources. The sources within each cluster are located within 10-15 km distance and the OMI spatial resolution is not fine enough to distinguish them as individual source. Therefore, we combined sources 1 and 2 as cluster 1, sources 3, 4 and 5 as cluster 2 and source 6 as cluster 3. The extensive use of ceramic products as structural materials and for decorative purposes in buildings has dramatically increased manufacturing in recent years (Sawdust, 2019), which has increased SO_2 emissions as shown in Figure 5. We found that emissions from Morbi ceramic industries have been near or above 100 kt y^{-1} since 2009. They are now comparable with the sum of emissions from sources in cluster 2 (i.e., Sikka Thermal Power Station (source 3), Essar oil refinery (source 4) and Jamnagar refinery (source 5)) and represent ~half of the total emissions from sources in cluster 1 (i.e., MTPS and UMPP (source 1) and Mundra port (source 2)). The SO_2 emissions from ceramic industries at Morbi are ~5 times higher in 2017 compared to 2005. The emissions from cluster 1 are ~2.75 times higher in 2017 compared to 2012, and cluster 2 are ~2.5 times higher in 2017 compared with 2005.

We examined global emissions inventories, such as Hemispheric Transport of Air Pollutants (HTAP) (Janssens-Maenhout et al., 2015), Emissions Database for Global Atmospheric Research (EDGAR, Janssens-Maenhout et al., 2013) and the MACCity inventory (Lamarque et al., 2010; Granier et al., 2011) and none of them report any significant SO_2 emissions from the grid cell closest to the Morbi area. While emission estimates for the ceramic industries near Morbi are not available, there are estimates of SO_2 emissions for MTPS. A recent study by Tong et al. (2018) estimated that SO_2 emissions from one of MTPS's power-generating units, of 330 MW capacity, were ~7.9 kt per year in 2010. As mentioned above, there were nine operational units in 2012 (4 units of 330 MW and 5 units of 660 MW) (Power Technology, 2019). This suggests that MTPS's SO_2 emissions were ~110.6 kt per year in 2012, which is in line with OMI-based estimates (~110 kt y^{-1}±25 kt y^{-1}).

While in this study we focused on Gujarat, India, there are other regions in the world with a high concentration of ceramic industries. For example, the total production of the ceramic industry in the Foshan region of China is even larger that in Morbi (3.3 (http://www.recocera.com/ceramic-tile-production-base/) and 2.8 million square meter tiles per day (https://www.morbiceramicindustry.com/index.html) respectively). However, these Chinese ceramic

industries are in close proximity to power plants, which makes it impossible for OMI to separate emissions from ceramic industries and power plants there.

4. Conclusions

India's ceramic industry is an important source of anthropogenic SO_2 emissions that is not accounted for in common emissions inventories. Increase in India's population and rapid movement of dwellers from villages and towns to cities for job/livelihood is creating more demand for ceramic products, which is providing an additional growth opportunity for ceramic industries. In the absence of any other information, emission from the Morbi region, where about 80% of Indian ceramic industries are located, can be estimated using satellite data. They are computed to be ~100 kt y^{-1} since 2009, which is comparable with emissions from a large power plant or oil refinery. Since there are ~600 ceramic factories in the Morbi ceramic cluster, on average each coal-based ceramic factory emits ~0.17 kt of SO_2 per year. Since there is an additional ~20% ceramic production outside of the Morbi region, one would expect an additional ~20 kt y^{-1} in SO_2 emissions for a national total emission estimates of ~120 kt y^{-1}. These new satellite-derived estimates can be used to help make more informed decisions on impacts of SO_2 emissions from the ceramic industries, as well as from oil refineries and power plants, on environment and human health. For example, these new satellite estimates can be used to monitor the impact of policy regulations such as those recently (March 9th, 2019) issued by Gujarat Pollution Control Board (GPCB) to close Morbi based ceramic units that are running on coal gasifiers following the National Green Tribunal order (Daily News and Analysis, 2019; The Times of India, 2019).

Acknowledgements

We acknowledge the National Aeronautics and Space Administration (NASA) for the availability of OMI SO_2 tropospheric column data. The data used in this study can be made available on request (Shailesh K. Kharol and V. Fioletov, Environment and Climate Change Canada).

References

Bauduin, S., Clarisse, L., Clerbaux, C., Hurtmans, D., Coheur, P.-F., 2014. IASI observations of sulfur dioxide (SO_2) in the boundary layer of Norilsk. J. Geophys. Res. Atmos. 119, 4253–4263. https://doi.org/10.1002/2013JD021405.

Bauduin, S., Clarisse, L., Hadji-Lazaro, J., Theys, N., Clerbaux, C., Coheur, P.F., 2016. Retrieval of

near-surface sulfur dioxide (SO_2) concentrations at a global scale using IASI satellite observations. Atmos. Meas. Tech. 9, 721–740. https://doi.org/10.5194/amt-9-721-2016.

BEE, 2010. Bureau of Energy Efficiency. Detailed project report on kiln insulation improvement (Morbi ceramic cluster) (https://www.dcmsme.gov.in/reports/morviceramic/MRV_CRM_Kiln_Insulation_Improvement_MRV_CRM_KII_14.pdf).

Care Ratings, 2019. Indian Ceramic Tile Industry: Structural shift with focus on higher value added products (http://www.careratings.com/upload/NewsFiles/Studies/Indian%20Ceramic%20Tile%20Industry.pdf).

Carn, S.A., Fioletov, V.E., McLinden, C.A., Li, C., Krotkov, N.A., 2017. A decade of global volcanic SO_2 emissions measured from space. Sci. Rep. 7, 44095. https://doi.org/10.1038/srep44095.

Carn, S.A., Krueger, A.J., Krotkov, N.A., Gray, M.A., 2004. Fire at Iraqi sulfur plant emits SO_2 clouds detected by Earth Probe TOMS. Geophys. Res. Lett. 31, L19105. https://doi.org/10.1029/2004GL020719.

Carn, S.A., Krueger, A.J., Krotkov, N.A., Yang, K., Levelt, P.F., 2007. Sulfur dioxide emissions from Peruvian copper smelters detected by the Ozone Monitoring Instrument. Geophys. Res. Lett. 34, L09801. https://doi.org/10.1029/2006GL029020.

de Foy, B., Krotkov, N.A., Bei, N., Herndon, S.C., Huey, L.G., Martínez, A.P., Ruiz-Suárez, L.G., Wood, E.C., Zavala, M., Molina, L.T., Mart, A., 2009. Hit from both sides: Tracking industrial and volcanic plumes in Mexico City with surface measurements and OMI SO_2 retrievals during the MILAGRO field campaign. Atmos. Chem. Phys. 9, 9599–9617. https://doi.org/10.5194/acp-9-9599-2009.

Daily News and Analysis, 2019. NGT orders closure of polluting ceramic units in Morbi (https://www.dnaindia.com/ahmedabad/report-ngt-orders-closure-of-polluting-ceramic-units-in-morbi-2727148).

Dee, D. P., et al., 2011. The ERA-Interim reanalysis: Configuration and performance of the data assimilation system, Q. J. Roy. Meteor. Soc., 137, 553–597, https://doi.org/10.1002/qj.828, 2011.

Ernst & Young LLP, 2013. Market research to identify strategies for Italian companies to enter into Indian ceramic tile market (http://www.icrim.eu/wordpress/wp-content/uploads/2014/12/Market-research-to-identify-strategies-for-Italian-companies-to-enter-into-Indian-Ceramic-tile-market.pdf).

Essar Refinery, 2019. https://en.wikipedia.org/wiki/Essar_Refinery.

Fioletov, V., McLinden, C.A., Kharol, S.K., Krotkov, N.A., Li, C., Joiner, J., Moran, M.D., Vet, R., Visschedijk, A.J.H., Denier Van Der Gon, H.A.C., 2017. Multi-source SO_2 emission retrievals and consistency of satellite and surface measurements with reported emissions. Atmos. Chem. Phys. 17. https://doi.org/10.5194/acp-17-12597-2017.

Fioletov, V.E., McLinden, C.A., Krotkov, N.A., Li, C., 2015. Lifetimes and emissions of SO_2 from point sources estimated from OMI. Geophys. Res. Lett. 42, 1–8. https://doi.org/10.1002/2015GL063148.

366 Fioletov, V.E., McLinden, C.A., Krotkov, N.A., Li, C., Joiner, J., Theys, N., Carn, S., Moran, M.D.,
367 2016. A global catalogue of large SO_2 sources and emissions derived from Ozone Monitoring
368 Instrument. Atmos. Chem. Phys. 16, 11497–11519. https://doi.org/doi:10.5194/acp-16-11497-2016.

369 Fioletov, V.E., McLinden, C.A., Krotkov, N., Moran, M.D., Yang, K., 2011. Estimation of SO_2
370 emissions using OMI retrievals. Geophys. Res. Lett. 38, L21811.
371 https://doi.org/10.1029/2011GL049402.

372 Fioletov, V.E., McLinden, C.A., Krotkov, N., Yang, K., Loyola, D.G., Valks, P., Theys, N., Van
373 Roozendael, M., Nowlan, C.R., Chance, K., Liu, X., Lee, C., Martin, R. V., 2013. Application of
374 OMI, SCIAMACHY, and GOME-2 satellite SO_2 retrievals for detection of large emission sources.
375 J. Geophys. Res. Atmos. 118, 11,399-11,418. https://doi.org/10.1002/jgrd.50826.

376 Granier, C. et al., 2011. Evolution of anthropogenic and biomass burning emissions of air pollutants at
377 global and regional scales during the 1980–2010 period. Climatic Change 109, 163–190.

378 Jamnagar Refinery, 2019. https://en.wikipedia.org/wiki/Jamnagar_Refinery.

379 Janssens-Maenhout, G. et al., 2015. HTAP_v2: a mosaic of regional and global emission gridmaps for
380 2008 and 2010 to study hemispheric transport of air pollution. Atmos. Chem. Phys. 15, 11411–
381 11432.

382 Janssens-Maenhout, G., Pagliari, V., Guizzardi, D., Muntean, M., 2013. Global Emission Inventories in
383 the Emission Database for Global Atmospheric Research (EDGAR) Manual (I): Gridding: EDGAR
384 Emissions Distribution on Global Gridmaps JRC Report EUR 25785 EN;
385 http://dx.doi.org/10.2788/81454.

386 Jiang, J., Zha, Y., Gao, J., Jiang, J., 2012. Monitoring of SO_2 column concentration change over China
387 from Aura OMI data. Int. J. Remote Sens. 33, 1934–1942.
388 https://doi.org/10.1080/01431161.2011.603380.

389 KICT, 2019. Kandla International Container Terminal-Newsletter-V. Ceramic & Tiles: Outlook
390 (https://www.ict.in/kict/newsletter/assets/Files/Issue-V/KICT-Newsletter-V.pdf).

391 Kharol, S. K., McLinden, C. A., Sioris, C. E., Shephard, M. W., Fioletov, V., van Donkelaar, A., Philip,
392 S., Martin, R. V., 2017. OMI satellite observations of decadal changes in ground-level sulfur
393 dioxide over North America. Atmos. Chem. Phys., 17, 5921-5929. https://doi.org/10.5194/acp-17-
394 5921-2017.

395 Klimont, Z., Smith, S.J., Cofala, J., 2013. The last decade of global anthropogenic sulfur dioxide: 2000–
396 2011 emissions. Environ. Res. Lett. 8, 14003. https://doi.org/10.1088/1748-9326/8/1/014003.

397 Koukouli, M.E., Balis, D.S., van der A, R.J., Theys, N., Hedelt, P., Richter, A., Krotkov, N., Li, C.,
398 Taylor, M., 2016. Anthropogenic sulphur dioxide load over China as observed from different
399 satellite sensors. Atmos. Environ. 145, 45–59. https://doi.org/10.1016/j.atmosenv.2016.09.007.

400 Krotkov, N.A., McLinden, C.A., Li, C., Lamsal, L.N., Celarier, E.A., Marchenko, S. V., Swartz, W.H.,
401 Bucsela, E.J., Joiner, J., Duncan, B.N., Boersma, K.F., Veefkind, J.P., Levelt, P.F., Fioletov, V.E.,
402 Dickerson, R.R., He, H., Lu, Z., Streets, D.G., 2016. Aura OMI observations of regional SO_2 and
403 NO_2 pollution changes from 2005 to 2015. Atmos. Chem. Phys. 16, 4605–4629.

https://doi.org/10.5194/acp-16-4605-2016.

Krotkov, N. a., McClure, B., Dickerson, R.R., Carn, S. a., Li, C., Bhartia, P.K., Yang, K., Krueger, A.J., Li, Z., Levelt, P.F., Chen, H., Wang, P., Lu, D., 2008. Validation of SO_2 retrievals from the Ozone Monitoring Instrument over NE China. J. Geophys. Res. 113, D16S40. https://doi.org/10.1029/2007JD008818.

Lamarque, J.-F., Bond, T. C., Eyring, V., Granier, C., Heil, A., Klimont, Z., Lee, D., Liousse, C., Mieville, A., Owen, B., Schultz, M. G., Shindell, D., Smith, S. J., Stehfest, E., Van Aardenne, J., Cooper, O. R., Kainuma, M., Mahowald, N., McConnell, J. R., Naik, V., Riahi, K., van Vuuren, D. P., 2010. Historical (1850–2000) gridded anthropogenic and biomass burning emissions of reactive gases and aerosols: methodology and application, Atmos. Chem. Phys. 10, 7017-7039, https://doi.org/10.5194/acp-10-7017-2010.

Lee, C., Martin, R. V., van Donkelaar, A., O'Byrne, G., Krotkov, N., Richter, A., Huey, L.G., Holloway, J.S., 2009. Retrieval of vertical columns of sulfur dioxide from SCIAMACHY and OMI: Air mass factor algorithm development, validation, and error analysis. J. Geophys. Res. 114, D22303. https://doi.org/10.1029/2009JD012123.

Levelt, P.F., Joiner, J., Tamminen, J., Veefkind, J.P., Bhartia, P.K., Fioletov, V., Carn, S., Laat, J. De, Deland, M., Marchenko, S., Mcpeters, R., 2018. The Ozone Monitoring Instrument : overview of 14 years in space. Atmos. Chem. Phys 18, 5699–5745. https://doi.org/https://doi.org/10.5194/acp-18-5699-2018.

Levelt, P.F., van den Oord, G.H.J., Dobber, M.R., Malkki, A., Stammes, P., Lundell, J.O.V., Saari, H., 2006. The Ozone Monitoring Instrument. IEEE Trans. Geosci. Remote Sens. 44, 1093–1101. https://doi.org/10.1109/TGRS.2006.872333.

Li, C., Joiner, J., Krotkov, N.A., Bhartia, P.K., 2013. A fast and sensitive new satellite SO_2 retrieval algorithm based on principal component analysis: Application to the ozone monitoring instrument. Geophys. Res. Lett. 40, 6314–6318. https://doi.org/10.1002/2013GL058134.

Li, C., McLinden, C., Fioletov, V., Krotkov, N., Carn, S., Joiner, J., Streets, D., He, H., Ren, X., Li, Z., Dickerson, R.R., 2017. India Is Overtaking China as the World's Largest Emitter of Anthropogenic Sulfur Dioxide. Sci. Rep. 7, 14304. https://doi.org/10.1038/s41598-017-14639-8.

Li, C., Zhang, Q., Krotkov, N.A., Streets, D.G., He, K., Tsay, S.-C., Gleason, J.F., 2010. Recent large reduction in sulfur dioxide emissions from Chinese power plants observed by the Ozone Monitoring Instrument. Geophys. Res. Lett. 37. https://doi.org/10.1029/2010GL042594.

Liu, F., Choi, S., Li, C., Fioletov, V. E., McLinden, C. A., Joiner, J., Krotkov, N. A., Bian, H., Janssens-Maenhout, G., Darmenov, A. S., and da Silva, A. M.: A new global anthropogenic SO_2 emission inventory for the last decade: a mosaic of satellite-derived and bottom-up emissions, Atmos. Chem. Phys., 18, 16571-16586, https://doi.org/10.5194/acp-18-16571-2018, 2018.

Lu, Z., Streets, D.G., De Foy, B., Krotkov, N.A., 2013. Ozone monitoring instrument observations of interannual increases in SO_2 emissions from Indian coal-fired power plants during 2005-2012. Environ. Sci. Technol. 47, 13993–14000. https://doi.org/10.1021/es4039648.

McLinden, C.A., Fioletov, V., Boersma, K.F., Kharol, S.K., Krotkov, N., Lamsal, L., Makar, P.A., Martin, R. V., Veefkind, J.P., Yang, K., 2014. Improved satellite retrievals of NO_2 and SO_2 over the Canadian oil sands and comparisons with surface measurements. Atmos. Chem. Phys. 14, 3637–3656. https://doi.org/10.5194/acp-14-3637-2014.

McLinden, C.A., Fioletov, V., Boersma, K.F., Krotkov, N., Sioris, C.E., Veefkind, J.P., Yang, K., 2012. Air quality over the Canadian oil sands: A first assessment using satellite observations. Geophys. Res. Lett. 39, 1–8. https://doi.org/10.1029/2011GL050273.

Mundra Port, 2019. https://en.wikipedia.org/wiki/Mundra_Port.

Nowlan, C.R., Liu, X., Chance, K., Cai, Z., Kurosu, T.P., Lee, C., Martin, R. V., 2011. Retrievals of sulfur dioxide from the Global Ozone Monitoring Experiment 2 (GOME-2) using an optimal estimation approach: Algorithm and initial validation. J. Geophys. Res. 116, D18301. https://doi.org/10.1029/2011JD015808.

Power Technology, 2019. The top 10 biggest thermal power plants in India (https://www.power-technology.com/features/feature-the-top-10-biggest-thermal-power-plants-in-india/).

Sawdust, 2019. Indian ceramics industry - growing in size (https://www.sawdust.online/reports/indian-ceramics-industry-growing-in-size/).

Seabrook, J. A., Smith, A., Clark, A. F., Gilliland, J. A., 2019. Geospatial analyses of adverse birth outcomes in Southwestern Ontario: Examining the impact of environmental factors. Environ. Res. 172, 18-26.

Schoeberl, M.R., Douglass, A.R., Hilsenrath, E., Bhartia, P.K., Beer, R., Waters, J.W., Gunson, M.R., Froidevaux, L., Gille, J.C., Barnett, J.J., Levelt, P.F., DeCola, P., 2006. Overview of the EOS Aura mission. IEEE Trans. Geosci. Remote Sens. 44, 1066–1074. https://doi.org/10.1109/TGRS.2005.861950.

Sikka Thermal Power Station, 2019. (https://en.wikipedia.org/wiki/Sikka_Thermal_Power_Station). Gujarat State Electricity Corporation Limited.

Theys, N., Smedt, I. De, Gent, J. Van, Danckaert, T., Wang, T., Hendrick, F., Stavrakou, T., Bauduin, S., Clarisse, L., Li, C., Krotkov, N., Yu, H., Brenot, H., Roozendael, M. Van, 2015. Sulfur dioxide vertical column DOAS retrievals from the Ozone Monitoring Instrument: Global observations and comparison to ground-based and satellite data. J. Geophys. Res. 120, 2470–2491. https://doi.org/10.1002/2014JD022657.

The Times of India, 2019. Closure notice to 550 Morbi ceramic units (https://timesofindia.indiatimes.com/city/ahmedabad/closure-notice-to-550-morbi-ceramic-units/articleshow/68340400.cms).

Thomas, W., Erbertseder, T., Ruppert, T., Roozendael, M. Van, Verdebout, J., Balis, D., Meleti, C., Zerefos, C., 2005. On the retrieval of volcanic sulfur dioxide emissions from GOME backscatter measurements. J. Atmos. Chem. 50, 295–320. https://doi.org/10.1007/s10874-005-5544-1.

Tong, D., Zhang, Q., Davis, S. J., Liu, F., Zheng, B., Geng, G., Xue, T., Li, M., Hong, C., Lu, Z., Streets, D. G., Guan, D., He, K., 2018. Targeted emission reductions from global super-polluting

power plant units. Nature Sustainability, 1, 59-68. https://doi.org/10.1038/s41893-017-0003-y.

Wen, D.Z., Kuang, Y.W., Liu, S.Z., Zhang, D.Q., Lu, Y.D., Li, J.L., 2006. Evidences and implications of vegetation damage from ceramic industrial emission on a rural site in the Pearl River Delta of China. J. of For. Res. 17(1),7-12. https://doi.org/10.1007/s11676-006-0002-8.

Witte, J.C., Schoeberl, M.R., Douglass, A.R., Gleason, J.F., Krotkov, N.A., Gille, J.C., Pickering, K.E., Livesey, N., 2009. Satellite observations of changes in air quality during the 2008 Beijing Olympics and Paralympics. Geophys. Res. Lett. 36, L17803. https://doi.org/10.1029/2009GL039236.

World's largest refineries, 2016. https://www.oilandgasclub.com/worlds-largest-refineries/. 9 September, 2016.

Highlights:

- First satellite estimates of SO_2 emissions from India's Morbi ceramic industry.
- SO_2 ceramic emissions are similar to those from large refineries and power plants.
- Morbi ceramic SO_2 emissions are ~5 times higher in 2017 compared to 2005.

Declaration of interests

☒ The authors declare that they have no known competing financial interests or personal relationships that could have appeared to influence the work reported in this paper.

☐The authors declare the following financial interests/personal relationships which may be considered as potential competing interests: